DFT Study of the NMR Properties of Xenon in Covalent Compounds and van der Waals Complexes—Implications for the Use of ^{129}Xe as a Molecular Probe

Alessandro Bagno*[a] and Giacomo Saielli[b]

Abstract: The NMR properties (chemical shift and spin–spin coupling constants) of ^{129}Xe in covalent compounds and weakly bound complexes have been investigated by DFT methods including relativistic effects. For covalent species, a good agreement between experimental and calculated results is achieved without scalar relativistic effects, but their inclusion (with a triple-ζ, double-polarization basis set) leads to some improvement in the quality of the correlation. The spin–orbit coupling term has a significant effect on the shielding constant, but makes a small contribution to the chemical shift. Coupling constants contain substantial contributions from the Fermi contact and paramagnetic spin–orbit terms; unlike light nuclei the spin–dipole term is also large, whereas the diamagnetic spin–orbit term is negligible. For van der Waals dimers, the dependence of the xenon chemical shift and anisotropy is calculated as a function of the distance. Small (<1 Hz) but non-negligible through-space coupling constants between ^{129}Xe and ^{13}C or ^{1}H are predicted. Much larger couplings, of the order of few Hz, are calculated between xenon and ^{17}O in a model silicate residue.

Keywords: density functional calculations · NMR spectroscopy · spin–spin coupling · van der Waals interaction · xenon

Introduction

The noble gas xenon has found widespread use as a molecular probe, owing to its low chemical reactivity and to the favorable NMR properties of the naturally occurring ^{129}Xe isotope (natural abundance 26.44%, $I=½$, $\gamma=-7.4521\times10^{7}$ rad s^{-1} T^{-1}), which render its observation relatively easy. More importantly, ^{129}Xe chemical shifts are sensitive to even tiny changes in the surroundings.[1] The scope of application of the xenon probe has received further strong impetus by exploiting the enormous NOE effects that can be achieved through hyperpolarization by optical laser pumping, taking advantage of its very slow intermolecular spin-lattice relaxation.[2] The other NMR-active isotope (^{131}Xe, $I=3/2$) has received less attention, although it is also finding use as molecular probe by techniques appropriate for quadrupolar nuclei.[3]

Among many examples of the use of ^{129}Xe as NMR probe, we will mention a few general areas. a) Study of the pore structure and adsorption properties of zeolites, since the position and width of ^{129}Xe lines depend on the interaction of Xe atoms with one another and with the pore walls.[4–6] Along with experimental investigations, computer simulations have been used in order to get atomic-level information of the arrangement of xenon atoms in zeolitic pores[6–8] and other porous materials.[9] b) Study of the ordering properties of liquid crystals: when dissolved in an anisotropic environment it is possible to observe the induced anisotropy of the shielding tensor and, therefore, to obtain information on the degree of order of the liquid crystalline material.[10] c) Study of proteins in aqueous solutions,[11] where nonspecific xenon–protein interaction can reveal conformational changes in the protein structure. d) Investigation of xenon–membrane interaction:[12] xenon is finding use as anaesthetic in medicine, and the interaction of xenon with lipids has received much attention because hyperpolarized ^{129}Xe can be dissolved in biologically compatible lipid emulsions while maintaining sufficient polarization for in vivo vascular imaging.[13] e) Exploiting isotope shifts of xenon caged in a deuterated cryptophane.[14] f) Study of Xe@C_{60}, for which an experimental ^{129}Xe NMR spectrum has been obtained.[15]

[a] Prof. A. Bagno
Dipartimento di Chimica Organica
Università di Padova
Via Marzolo, 1, 35131 Padova (Italy)
Fax: (+39) 0498275239
E-mail: alessandro.bagno@unipd.it

[b] Dr. G. Saielli
Istituto per la Tecnologia delle Membrane—CNR
Sezione di Padova, Via Marzolo, 1, 35131 Padova (Italy)

Supporting information for this article is available on the WWW under http://www.chemeurj.org or from the author.

0947-6539/03/0907-1486 $ 20.00+.50/0 *Chem. Eur. J.* **2003**, *9*, No. 7

Despite its widespread use, quantum chemical characterization and predictions of the NMR properties of ^{129}Xe (as free atom, in covalent compounds or weakly bound complexes), are limited.[16, 17] Among these, we note that GIAO-HF calculations of xenon shifts in $Xe@C_{60}$, as well as an MP2 calculation for the Xe···benzene complex at a selected distance, have been reported.[18] Recently, the HF-level calculation of xenon shifts in xenon dimers and other simple van der Waals complexes have also been reported,[19] with the aim of modelling the NMR properties of xenon in nanochannels. Similarily, chemical shift for xenon adsorbed on molecular sieves were reported, based on model Xe···Xe and Xe···H_2O dimers.[20] Also, the calculation of spin–spin couplings in Xe···Xe and Xe···H dimers, based on a variant of density functional theory[21] was presented. These data had previously prompted us to investigate the transmission of spin–spin coupling through space in van der Waals dimers.[22] Our results, as well as those by other groups, consistently indicated an almost ubiquitous occurrence of through-space or through-hydrogen-bond couplings for several pairs of nuclei (notably $^1H-^{13}C$ and $^1H-^{19}F$, where they may be far from small[23, 24]). Finally, $^1J_{Xe,F}$ for some xenon fluorides from relativistic DFT calculations have been recently reported.[25]

The observation of through-space couplings involving xenon would have important consequences. The existence of scalar coupling is normally taken as strong evidence of chemical bonding. In weakly dispersion-bound complexes there is, obviously, no such implication; however, the rapid decay of calculated values with increasing distance (see e.g.[22, 26]) renders this quantity a sensitive probe of spatial proximity akin to the NOE. In other words, the strong structural information that it carries would in fact allow one to map specific probe-pore/channel interactions at atomic level. Thus, the capability to predict such through-space couplings may be viewed as a guideline for tailoring NMR experiments to hopefully observe this phenomenon.

Prompted by the increasing scope of application of xenon as probe, we have endeavored to provide a comprehensive set of calculations to predict its relevant NMR parameters. Given the scarcity of such calculations, in this paper we firstly validate the methodology by investigating the NMR properties of xenon in covalent compounds. We then turn our attention to weakly bound complexes, for which hardly any experimental data are available for direct comparison. Van der Waals complexes are chosen so as to represent model systems of the weak interactions of xenon in common environments such as zeolites, liquid crystals, cryptophanes. In these cases the analysis of the calculated chemical shift and shielding anisotropy, as well as the through-space coupling, will serve as a tool to rationalize experimental observations and hopefully to enable the prediction of these NMR parameters.

Computational Methods

The calculation of NMR properties has been carried out using density functional theory (DFT) as implemented in the Amsterdam Density Functional (ADF) code,[27] in which frozen-core, as well as all-electron, Slater basis sets are available for all atoms. The most frequently used basis set in this work was the triple-ζ, double-polarization TZ2P, including functions up to 5d and 4f for Xe. Relativistic frozen-core potentials for relativistic calculations (not to be confused with effective core potential basis sets), required to run ZORA calculations, were generated with the Dirac utility.[27] The ADF code also offers the possibility of taking relativistic effects into account, by means of the Pauli method, or the more recent, recommended two-component zero-order regular approximation (ZORA) method, which requires specially optimized basis sets. It is possible to include either only the scalar (Darwin and mass-velocity) correction or spin–orbit coupling too. The ADF NMR property modules allow for the calculation of nuclear shieldings and spin–spin couplings by the ZORA method. Details about theory and implementation are described in refs. [28, 29]. The nonrelativistic contribution to the spin–spin coupling obtained by Ramsey,[30] that is the Fermi-Contact (FC), diamagnetic spin-orbit (DSO), paramagnetic spin-orbit (PSO) and spin-dipole (SD) can be also derived within the relativistic approximation, although the ZORA terms are somewhat different.[28, 29]

Ziegler and co-workers have carried out broad computational investigations of heavy-atom nuclei (e.g. ^{183}W, ^{195}Pt, ^{199}Hg, ^{205}Tl, ^{207}Pb, ^{235}U), and observed large relativistic effects on their NMR properties.[31] For lighter atoms such as Xe, these effects on NMR parameters may still be substantial since both the shielding and the coupling constant involve core orbitals (or the core tails of valence orbitals). Whether these effects show up or not depends, to some extent, on the fact that chemical shifts are the difference between the shieldings in two species, implying that they may partly cancel. Thus, for example, an excellent agreement between experimental ^{99}Ru chemical shifts and nonrelativistic calculated values was obtained.[32] This will not be the case if one or more 3rd- or 4th-row atoms, typically iodine, are bonded to the observed NMR nucleus and the bond has a high *s* character, where spin–orbit coupling makes a large contribution to the overall shielding.[33, 34] Even though this investigation involves only light atoms bonded to Xe, the limited knowledge base concerning spin–orbit effects prompted us to determine the relevance of relativistic effects in the calculated NMR properties of xenon.

With regard to weak dispersion-bound complexes, since DFT may not treat the energetics of this interaction correctly, we have evaluated the interaction energies by the MP2 ab initio method, with the DZVP[35] Gaussian basis set for all atoms, using Gaussian 98.[36] Energies were corrected for basis set superposition error (BSSE) by the counterpoise method.[37] In order to assess the basis-set effect, we also ran a corresponding set of calculations for two test cases (Xe dimer and Xe–benzene complex) with the recently defined[38] SDB-cc-pVTZ basis, which includes an effective-core potential for xenon.

Results and Discussion

Covalent compounds: Among the noble gases, xenon features the largest number of covalent compounds known, most of which are binary or ternary species where xenon is bonded to F, O or N. Although many such species are unstable, for a fair number of them a high-resolution ^{129}Xe spectrum is available, from which accurate chemical shifts and coupling constants can be extracted. The whole known shielding range, even within the limited structural variability allowed, amounts to more than 7000 ppm (free Xe being the most shielded at $\delta = -5331$, up to XeO_6^{4-} at $\delta = +2077$), that is, the typical range for nuclei of this atomic number. A strong dependence of the chemical shift on the oxidation state is known; noticeable temperature and solvent effects are also found, whereby experimental values often span a rather broad interval. Nevertheless, the wide experimental window of data make xenon a suitable candidate to test the performance of density functional calculations. We have investigated the covalent compounds listed in Tables 1 and 2, below, where we report

  0947-6539/03/0907-1487 $ 20.00+.50/0

the experimental results for the chemical shift (relative to the commonly accepted standard $XeOF_4$), and coupling constants.[1] Spin–spin couplings to ^{129}Xe involve the typical nuclides ^{35}Cl, ^{29}Si, ^{19}F, ^{17}O, ^{15}N, ^{13}C, ^{1}H. The structures of most compounds considered in the calculations were obtained from X-ray experimental data as reported in Table 1. For some species (XeF_6, XeF^+, $XeCl^+$) the solution structure is uncertain, and neither the calculated chemical shift and, especially, the couplings satisfactorily correlated with the experimental data. These compounds will be dealt with separately, and the results are not included in the fitting of the calculated versus experimental data.

The results of the calculations are the components of the Xe shielding tensor $\boldsymbol{\sigma}$, that is, the diamagnetic term σ_d, the paramagnetic term σ_p and, for the relativistic spin–orbit approximation, also the spin–orbit term, σ_{SO}. The chemical shift δ is calculated from the isotropic component σ of the shielding tensor as $\delta = \sigma_{ref} - \sigma$ where σ_{ref} refers to $XeOF_4$. The other property of interest that we calculated is the spin–spin coupling constant between xenon and the other NMR-active nuclei in the molecule. The total coupling tensor $\boldsymbol{J}$ is obtained as a sum of the four constituent contributions, as already mentioned: FC, DSO, PSO and SD. At the spin–orbit ZORA level, apart from the DSO contribution, only the sum (FC+SD) can be determined along with PSO, each containing cross terms with the other. We are only interested in the isotropic component of the shielding and coupling tensors, since the anisotropic part is averaged to zero in isotropic solution due to the rapid tumbling motion.

As a preliminary test we investigated the effect of some of the functionals available in ADF, namely Perdew–Wang 91,[52] Perdew–Burke–Ernzerhof 96,[53] the PBE revised by Hammer–Hansen–Norskov,[54] the PBE revised by Zhang and Wang,[55] the Becke 88 exchange[56] plus Lee–Yang–Parr correlation,[57] and the Becke 88 exchange[56] plus the Perdew 86 correlation[58] (BP). This was done by calculating the $^1J_{Xe,F}$ and $^1J_{Xe,O}$ coupling constants (apparently the most-demanding properties) in $XeOF_4$ at the nonrelativistic level, with the TZP basis set Xe.4p for xenon and all-electron for O and F. We did not find any functional to perform systematically better than any other (Table S1 of the Supporting Information); we therefore chose the BP functional for all subsequent calculations. We also performed some further tests to investigate the basis set effect. Thus, we ran a series of calculations of $^1J_{Xe,F}$ in XeF_2 and XeF_4 at the scalar ZORA level with the all-electron DZ, TZP, TZ2P and QZ4P basis sets defined in ADF. We found a systematic improvement of the results up to the TZ2P basis set, while the effect of the larger and computationally quite expensive QZ4P appears to be difficult to assess (Table S2 in the Supporting Information). We therefore decided to use the TZ2P basis for all our relativistic calculations, and the TZP basis for the nonrelativistic ones. The choice was dictated by the fact that the all-electron TZ2P basis set for xenon is only available for ZORA calculations.

An additional test was run to compare the performance of ab initio and DFT nonrelativistic calculations. Thus, in Figure 1 and Table S3 we report the results for few cases (Xe, XeF_2, XeF_4, $XeOF_4$) with two such methods, that is,

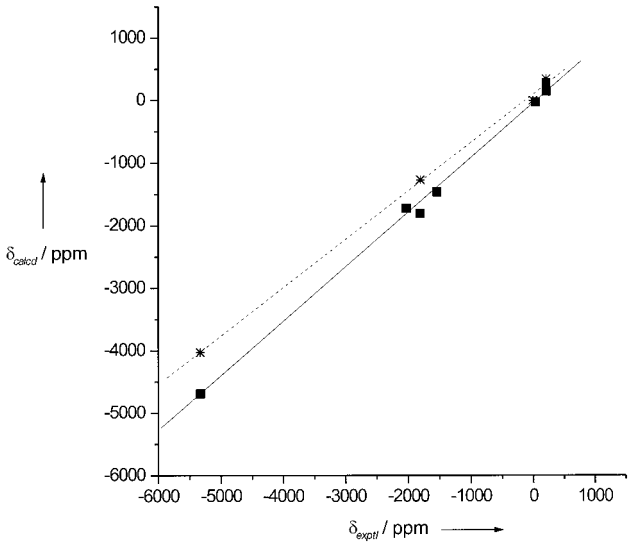

Figure 1. Correlation between experimental and calculated chemical shifts relative to $XeOF_4$ (δ, ppm) from nonrelativistic calculations. MP2/DZVP (*, ----); BP/TZP (■, ——).

MP2/DZVP and BP/TZP with frozen core up to 4p for xenon (Xe.4p) and all-electron for light atoms. The linear fit ($a+bx$) of calculated versus experimental δ yielded $a = 100$, $b = 0.77$, $r = 0.999$ (MP2) and $a = -42$, $b = 0.87$, $r = 0.996$ (DFT). Hence, the outcome is rather similar, in that MP2 results show a slightly better correlation but with a slope farther from unity. However, the computational cost of MP2 shielding calculations increases dramatically for species bigger than $XeOF_4$, and this approach was not further pursued.

In the following we report the results obtained at the three levels of theory employed for covalent compounds. a) Nonrelativistic, b) relativistic scalar ZORA and c) relativistic spin–orbit ZORA. At the nonrelativistic level we used the frozen core Xe.4p basis set for xenon and all-electron basis sets for the light atoms. At the relativistic spin–orbit level we used the TZ2P all-electron basis on all atoms, while at the intermediate relativistic scalar level we ran calculations with both basis sets. Whenever a range of experimental data was available, we considered the mean value. For brevity, we will report in detail only the results obtained at the scalar ZORA/TZ2P level; the nonrelativistic and relativistic spin–orbit level results are available as Supporting Information (Tables S3–S6).

At the nonrelativistic level σ_d is almost constant, while σ_p is strongly dependent on the oxidation state. Owing to its spherical symmetry, for the free xenon atom σ_p is exactly zero at the nonrelativistic level (and very small at relativistic levels) and accordingly the free atom turns out to be the most shielded. Covalent compounds are much less shielded in the order $Xe^{II} < Xe^{IV} < Xe^{VI}$, in agreement with experiment. With regard to spin–spin couplings, we observe that the FC contribution is not dominant, since the PSO term is of comparable magnitude or even larger. The SD term is also very important, especially for $^1J_{Xe,F}$ couplings, while the DSO term is negligible, being always less than 0.1% of the total coupling (this applies also to relativistic results, so it will not be further reported). The correlation between the calculated

0947-6539/03/0907-1488 $ 20.00+.50/0 *Chem. Eur. J.* **2003**, *9*, No. 7

and experimental results for the chemical shift is rather good, since only the chemical shift of xenon atom does not fit well in the correlation. The linear fit ($a+bx$) of calculated versus experimental δ yielded $a=-41.8$, $b=0.87$, and correlation coefficient $r=0.997$. The correlation between spin–spin couplings is also good, as can be appreciated from the fit parameters: $a=-126.4$, $b=0.96$, $r=0.994$. Hence, nonrelativistic calculations underestimate shifts and couplings by 4–13%. Including the scalar relativistic effects, but with the same basis set (TZP-Xe.4p) led to somewhat worse results.

Therefore we ran calculations at the relativistic scalar ZORA approximation with the TZ2P all-electron basis set. The results of shielding calculations are reported in Table 1; in Figure 2a we report the correlation between experimental and calculated chemical shifts.

Table 1. Calculated and experimental ^{129}Xe nuclear shieldings and chemical shifts [ppm] at the scalar ZORA/TZ2P level.

Species	σ_p	σ_d	σ	δ_{calcd}	δ_{exptl}	Ref.
Xe	82	5578	5660	−5414	−5331	[1]
XeF_2	−3478	5571	2093	−1847	−1592; −2009	[44,45]
$FXeOSO_2F$	−3753	5572	1818	−1572	−1407; −1666	[47]
$FXeN(SO_2F)_2$	−3420	5572	2152	−1906	−1997; −2053	[50][a]
XeF_4	−5880	5565	−315	561	166.1; 259	[44,45]
XeO_2F_2	−5239	5571	332	−86	17; 73	[46,48]
$XeOF_4$	−5320	5566	246	0	0	[44,45]
XeO_3	−5395	5575	180	66	217	[49]
XeF_6	−5387	5561	174	72	−35; −45	[39–42]
XeF^+	−7458	5570	−1888	2134[b]	−574; −911	[43]
$Xe_2F_3^+$	−4557	5570	1013	−767		[51]
$XeCl^+$	−2276	5574	3298	−3052[c]	−551	[43]

[a] The geometry used in the calculations was obtained by optimization at the scalar ZORA/TZ2P level, starting from the experimental structure. The average difference in bonds lengths and angles is 0.016 Å and 1°, respectively. [b] $\delta=705$ ppm at the ZORA spin–orbit/TZ2P level. [c] $\delta=-3551$ ppm at the ZORA spin–orbit level.

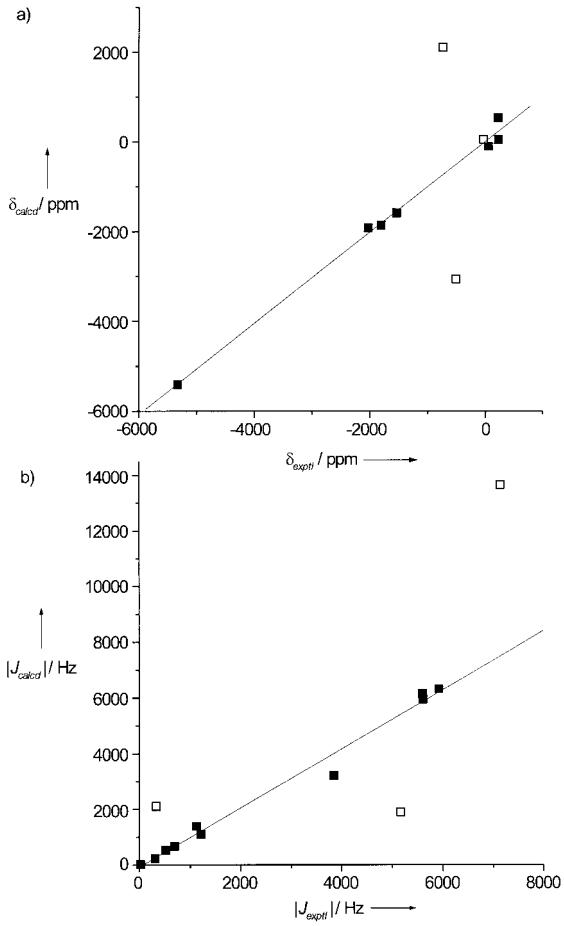

Figure 2. Correlation between experimental and calculated NMR parameters (Tables 1 and 2). a) Chemical shifts relative to $XeOF_4$ (δ, ppm) at the scalar ZORA/TZ2P level. The data points for XeF^+, $XeCl^+$ and XeF_6 (□) are not included in the fit (see text). b) Spin–spin couplings (J, Hz; absolute values).

We note an improvement on going from the nonrelativistic to the scalar relativistic case, as indicated by the slope b ($a=28$, $b=1.02$, $r=0.996$). In particular, the chemical shift of the xenon atom is in much better agreement. However, by comparing with the results seen above it is evident that this result is due to the larger basis set used, rather than to the inclusion of relativistic effects. In Figure 2b we report the correlation between experimental (absolute value) and calculated coupling constants (data in Table 2). For this property we did not find a significant improvement ($a=-79$; $b=1.06$; $r=0.993$). Actually, $^1J_{Xe,F}$ in XeF_4 shows a relatively large error of about 16%. In order to check whether this is due to a problem with the geometry, we ran a calculation for a structure optimized at the scalar ZORA/TZ2P level. The bond length changed from the experimental value[44] of 1.940 to 1.955 Å. However, the coupling constant at the optimized geometry was essentially unchanged.

At the spin–orbit relativistic ZORA/TZ2P level we found σ_{SO} to be quite significant, reaching up to about 30% of the total value. This contribution is, however, rather similar for most species (with a range of ca. 400 ppm), so that it partly cancels out in the resulting chemical shift, and δ values are not much affected by this contribution. This approach in fact gives a correlation of similar quality as the scalar one (chemical shifts: $a=-207$, $b=1.03$, $r=0.995$, coupling constants: $a=15$, $b=1.03$, $r=0.997$). $^1J_{Xe,F}$ in XeF_4 is now in better agreement with experiment; however, given that all other parameters are well reproduced at the scalar ZORA level, this may be fortuitous. Solvent coordination may also play a role, since XeF_4 is structurally related to other square-planar complexes for which similar problems were encountered.[31] Interestingly, the species with the largest σ_{SO} are XeF^+ and $XeCl^+$ (see below).

We note that a very good agreement was obtained[25] for $^1J_{Xe,F}$ in XeF_4 at this level of theory. However, the basis set has one polarization function (5d) less than the one included in the latest version of ADF.[27] Indeed, by using the same basis set we obtained the same result.

In conclusion, a good correlation between calculated and experimental NMR properties of xenon covalent compounds can be obtained at a nonrelativistic level using density functional theory with basis sets of moderate size and frozen core for xenon (TZP-Xe.4p). An almost quantitative agreement is found including scalar relativistic corrections with the larger all-electron TZ2P basis set, while the inclusion of the

  0947-6539/03/0907-1489 $ 20.00+.50/0

Table 2. Calculated and experimental coupling constants [Hz] at the scalar ZORA/TZ2P level.[a]

Species		PSO	FC	SD	J_{calcd}	$\lvert J_{exptl}\rvert$
XeF_2	$^1J_{Xe,F}$	−2979	−1998	−981	−5958	5550; 5665
$FxeOSO_2F$	$^1J_{Xe,F}$	−3472	−1758	−1090	−6320	5830; 6051
$FXeN(SO_2F)_2$	$^1J_{Xe,F}$	−3217	−1899	−1044	−6160	5572; 5624
	$^1J_{Xe,N}$	50.7	163.2	20.3	234	307.4
	$^3J_{Xe,F}$	6.7	−18.1	−4.9	−16.3	18
XeF_4	$^1J_{Xe,F}$	−258	−2587	−375	−3221	3801; 3900
XeO_2F_2	$^1J_{Xe,F}$	189	−1167	−129	−1107	1217
	$^1J_{Xe,O}$	−191	−343	11	−523	521
$XeOF_4$	$^1J_{Xe,F}$	456	−1717	−122	−1383	1115; 1131
	$^1J_{Xe,O}$	−235	−447	16	−665	692
XeF_6[b]	$^1J_{Xe,F}$	753	−2707	−150	−2104	330
XeF^+	$^1J_{Xe,F}$	−9436	−818	−3401	−13655[c]	6703; 7594
$Xe_2F_3^+$[d]	$^1J_{Xe,F1}$	−1492	3188	−426	−5107	
	$^1J_{Xe,F2}$	−4883	−1370	−1694	−7947	
	$^2J_{Xe,Xe}$	224	526	41	792	–
$XeCl^+$	$^1J_{Xe,Cl}$	−114	−1325	−460	−1899[e]	5165[f]

[a] See Table 1 for references to experimental values; all couplings reported as positive because the sign is not known. The DSO term is negligible. [b] Average of the results obtained for the two nonequivalent fluorine atoms in C_{3v} structure. [c] $J = -10302$ Hz at the ZORA spin–orbit level. [d] $F_{(2)}$-Xe-$F_{(1)}$-Xe-$F_{(2)}$. Average of $^1J_{Xe,F}$ couplings is −6527 Hz. [e] $J = -1519$ Hz at the ZORA spin–orbit level. [f] Separation between the two very broad (8 kHz) signals observed in the spectrum in HF/SbF_5.[43]

spin–orbit interaction does not markedly improve the results, although the shielding constant is strongly affected.

XeF_6 and ionic species: As mentioned above, for some species (XeF_6, XeF^+, $XeCl^+$) large deviations can be seen from the fitting line of Figure 1, and these discrepancies must be reconciled. We note in passing that spin–orbit coupling has a sizable effect (e.g., for XeF^+, δ goes from 2134 to 705 ppm, and $^1J_{Xe,F}$ from −13655 to −10302 Hz; see footnotes to Tables 1 and 2), but this correction is far from being sufficient to bring the calculated values into the target range; hence, we will again restrict the discussion to scalar ZORA results.

A major point to note is that there appears to be a large uncertainty with regard to the actual structure in solution, as summarized below.

For XeF_6, according to recent calculations,[39, 40] the most stable conformation in the gas phase has C_{3v} symmetry, whereas the octahedral one is calculated to be a transition state connecting two C_{3v} conformers. The calculation of NMR parameters was performed on the MP2 structure obtained in ref. [39], which resulted in a substantial discrepancy in $^1J_{Xe,F}$ (Table 2). However, it is not yet clear whether the solution structure is monomeric, or rather tetrameric or hexameric as postulated for the solid state.[41, 42] The large size and uncertain nature of these higher species prevented us from further pursuing the issue. However, given the good performance just seen for well-behaved compounds, this seems the most likely cause for the discrepancy and, indeed, the calculated values may be used as evidence indicating this structural change.

For XeF^+ experimental NMR data, obtained in superacid media (HF/SbF_5), are reported.[1] In such media, there is again some uncertainty as to the nature of the species, so that the disagreement probably stems from a substantial divergence with the structure considered in the computations. Given the coordinatively unsaturated nature of this species, strong interactions involving the counterion or other ions may be held responsible. The large discrepancy for coupling constants (calcd $^1J_{Xe,F} = -13.7$ kHz, exptl ca. 7 kHz) is suggestive; explicit inclusion of coordinated solvent molecules was found essential in order to acceptably calculate couplings for coordinatively unsaturated complexes such as MeHgX, $Hg(CN)_2$, $PtX_2(PMe_3)_2$ and $[(CN)_5Pt{-}Tl(CN)]^-$.[31]

The simplest species that XeF^+ can form in superacid solutions is probably $Xe_2F_3^+$, that is, a fluoride-bonded $[FXe{-}F{-}XeF]^+$ dimer, which was indeed postulated[45] as a possible actual structure of XeF^+ in such media. A calculation for $Xe_2F_3^+$ (Tables 1 and 2) yields a δ value (−767 ppm) quite consistent with the rather broad range of experimental values. The $^1J_{Xe,F}$ couplings are −5107 and −7947 Hz with the central and terminal fluorine atoms, respectively. Thus, apart from the sign, the average $^1J_{Xe,F} = -6527$ Hz agrees with the experimental values ranging between 6.7–7.6 kHz. (Incidentally, we note the substantial $^2J_{Xe,Xe}$ coupling of 792 Hz, which should be detectable in less symmetric adducts.)

The case of $XeCl^+$ deserves particular attention, since an experimental NMR spectrum has been carefully obtained very recently.[43] The NMR spectrum in HF/SbF_5 features two very broad (8 kHz) signals centered at $\delta = -551$ (calcd $\delta = -3052$), separated by 5165 Hz (calcd $^1J_{Xe,Cl} = -1899$ Hz). The line width and splitting were tentatively ascribed to coupling with $^{35,37}Cl$. Hence, there are major differences with the calculated values. Moreover, the large line broadening and multiplicity must also be accounted for. On the basis of the above results, we are inclined to believe that in superacid solution $XeCl^+$ may also be present as a bridged species of unknown nature. However, this statement must be strengthened by further results.[59]

Van der Waals dimers: We have studied the xenon dimer and the van der Waals complexes shown in Figure 3. The interaction energy was calculated with a step of 0.2 Å, at least

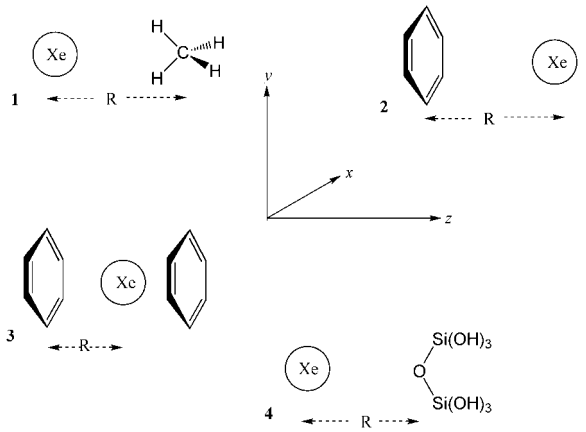

Figure 3. Xenon van der Waals complexes investigated.

around the minimum, and a cubic spline is used to determine the equilibrium distance r_{eq}, together with the energy stabilization at the equilibrium separation, ΔE.

All NMR properties have been calculated at the scalar ZORA/TZ2P level, in accord with our previous findings for

0947-6539/03/0907-1490 $ 20.00+.50/0 *Chem. Eur. J.* **2003**, *9*, No. 7

covalent species (and also because the larger QZ4P basis did not perform particularly well, besides its being too demanding for these systems). At variance with the preceding section, chemical shifts are given with respect to the free xenon atom, since this is the usual reference when xenon is used as probe, for example in zeolites and liquid crystals, and we will adopt this convention. In the paper, we will present these results only in a graphical form; the complete data are available as Supporting Information (Tables S7–S14). We have previously shown that ab initio and DFT methods perform similarly in the calculation of through-space couplings of organic van der Waals and CH/π interacting systems.[22]

The Xe···Xe dimer: The equilibrium distance ($r_{eq} = 4.93$ Å) is similar to the value of 4.98 Å obtained from DFT calculations using a functional specifically parameterized for van der Waals complexes.[60] The interaction energy ΔE, was calculated to be -0.16 kcal mol^{-1}. These results are quite at variance with the empirical Aziz–Slaman pair potential for xenon in the gas phase,[61] for which the equilibrium distance is 4.36 Å and the interaction energy at r_{eq} is -0.561 kcal mol^{-1}. In order to check for a possible basis set effect, we compared with the larger SDB-cc-pVTZ basis set (Figure 4), whereby

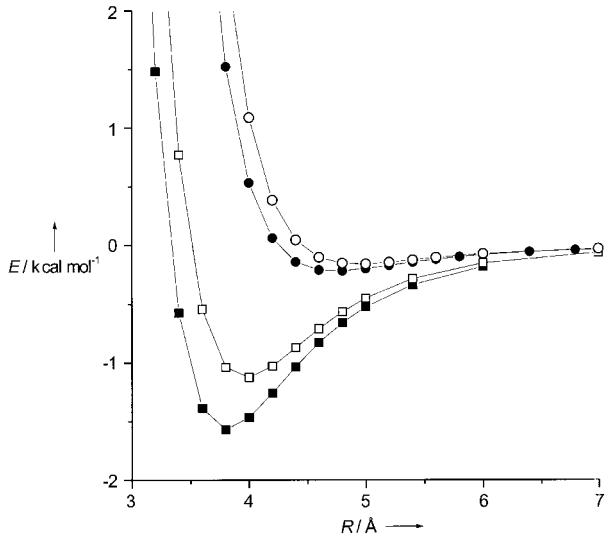

Figure 4. Basis-set effect on the energetics of interaction [kcal mol^{-1}] in xenon van der Waals complexes at the MP2 level with BSSE correction; empty and filled markers correspond to the DZVP and SDB-cc-pVTZ bases, respectively. Xenon dimer (circles); xenon-benzene complex (squares).

the energy minimum moves to shorter distances, and to more negative values, upon switching to the larger basis. The same trend is apparent also for the Xe–benzene complex. However, the change is relatively small, so this discrepancy might be attributed, for example, to the lack of diffuse functions in the basis sets. We may then safely assume that our equilibrium distances and interaction energies are underestimated; therefore, the true minimum is expected to occur for distances were shielding and especially through-space couplings are even larger.

In Figure 5a we report the xenon chemical shift δ, which shows a smooth increase from zero (at infinite distance) to positive shifts, amounting to about 10 ppm at r_{eq}.

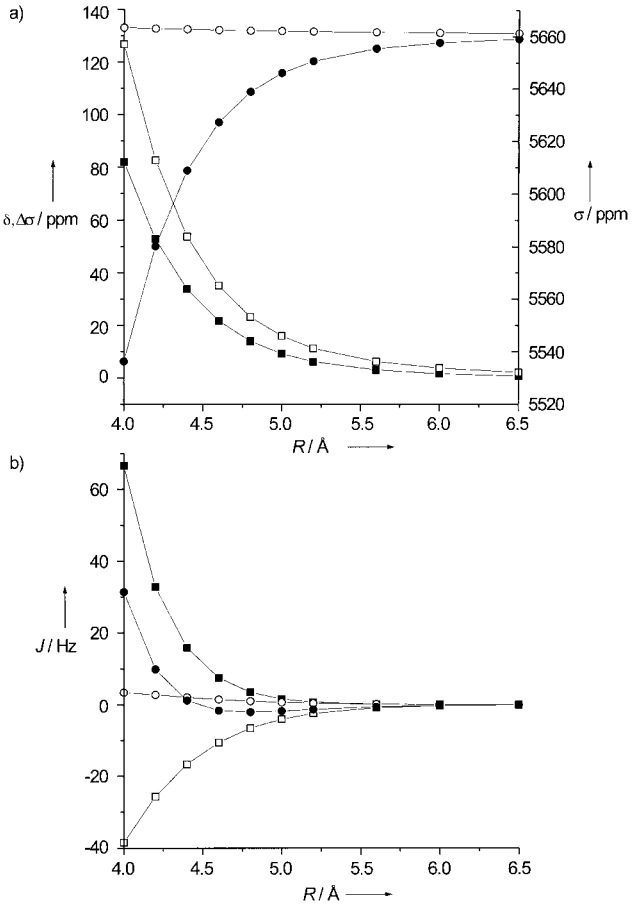

Figure 5. a) NMR shielding parameters of xenon in the Xe···Xe dimer. Left axis: chemical shift (■); shielding anisotropy (□). Right axis: the two components, $\sigma_{\parallel}$ (○) and $\sigma_{\perp}$ (●), of the xenon shielding tensor. b) Spin–spin coupling constant $J_{Xe,Xe}$ of the Xe···Xe dimer. PSO (□); FC (■); SD (○); total coupling (●). The DSO contribution is negligible.

In the same Figure we also show the anisotropy ($\Delta\sigma$) of the shielding tensor for a xenon atom of the dimer. Since the tensor has a cylindrical symmetry, the z axis lying along the internuclear vector, $\Delta\sigma = \sigma_{\parallel} - \sigma_{\perp}$, where $\sigma_{\parallel}$ is defined along the z axis, while $\sigma_{\perp}$ is the component in the perpendicular plane. As we can see in Figure 5a, $\sigma_{\parallel}$ is close to the isotropic value (5660 ppm) throughout the range investigated; almost all the isotropic chemical shift comes from a variation in $\sigma_{\perp}$. The results of Jameson and co-workers[19] are qualitatively in agreement with ours, although at the equilibrium separation the chemical shift at the DFT level is about twice as large as the HF result. The coupling constant, here assumed to be between two ^{129}Xe nuclei, is shown in Figure 5b. The DSO contribution is essentially negligible, as found previously for the covalent compounds. Although the PSO and FC terms are dominating, the SD contribution is not negligible. The total coupling constant in the region around the energy minimum is a few Hz, for example, -1.8 Hz at 5.0 Å, which corresponds to a reduced coupling constant $K = (4\pi^2/h)(J/\gamma_{Xe}{}^2)$ of -1.93×10^{19} kg m^{-2} C^{-2}. At about the same distance, the value of K calculated in ref. [21] (0.0155×10^{19} kg m^{-2} C^{-2}) is two orders of magnitude smaller.

The Xe···CH$_4$ complex (1): The system is defined such that the z axis is along the Xe–C direction, and the two closest

hydrogens lie in the yz plane. For this complex $r_{eq} = 4.73$ Å, with an interaction energy $\Delta E = -0.11$ kcal mol^{-1}. The behavior and the magnitude of the induced chemical shift and anisotropy is very similar to the previous case (see Figure 6a), with a chemical shift of about 10 ppm at r_{eq}.

The anisotropy is now defined as $\sigma_z - (\sigma_x + \sigma_y)/2$. The through-space $J_{Xe,C}$ couplings are reported in Figure 6b. The DSO term is, again, negligible and the SD contribution is also very small. The dominant contribution is represented by the FC term, with a significant contribution also from the PSO term. The coupling rapidly decays to zero with increasing the distance, and takes a value of about 0.18 Hz at a separation of 4.6 Å, a similar result to those found for the through-space couplings in CH/π systems.[22] At the same distance, the coupling with ^{1}H is significantly larger, -0.40 and -0.31 Hz with the two closest and the two farthest ones (Figure 3) respectively. $J_{Xe,H}$ is dominated by the FC term (Figure 6c).

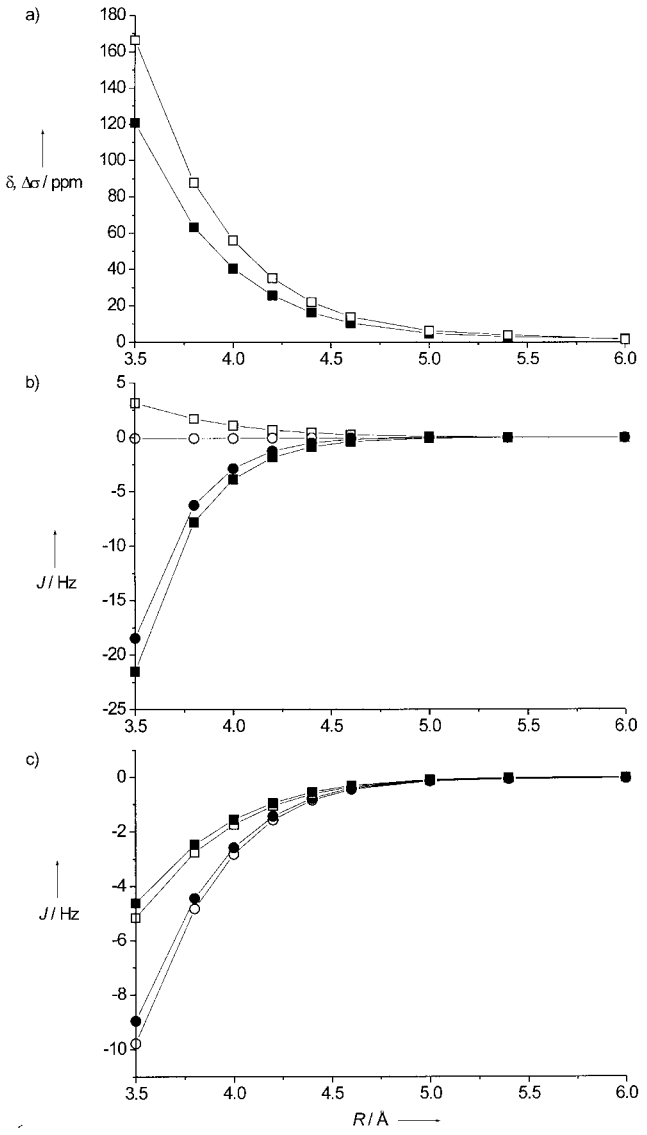

Figure 6. a) NMR shielding parameters of xenon in the Xe···CH_4 complex **1**. Chemical shift (■); shielding anisotropy (□). b) Coupling constant $J_{Xe,C}$. PSO (□); FC (■); SD (○); total coupling (●). The DSO contribution is negligible. c) Spin–spin coupling constant $J_{Xe,H}$: FC (□) and total coupling (■) with the closest hydrogens; FC (○) and total coupling (●) with the farthest hydrogens (see Figure 2).

The Xe···benzene complex (2): For the Xe–benzene complex **2** ($r_{eq} = 3.96$ Å, $\Delta E = -1.13$ kcal mol^{-1}), the results highlight a complex behavior of the chemical shift and shielding anisotropy as a function of the distance, as shown in Figure 7a.

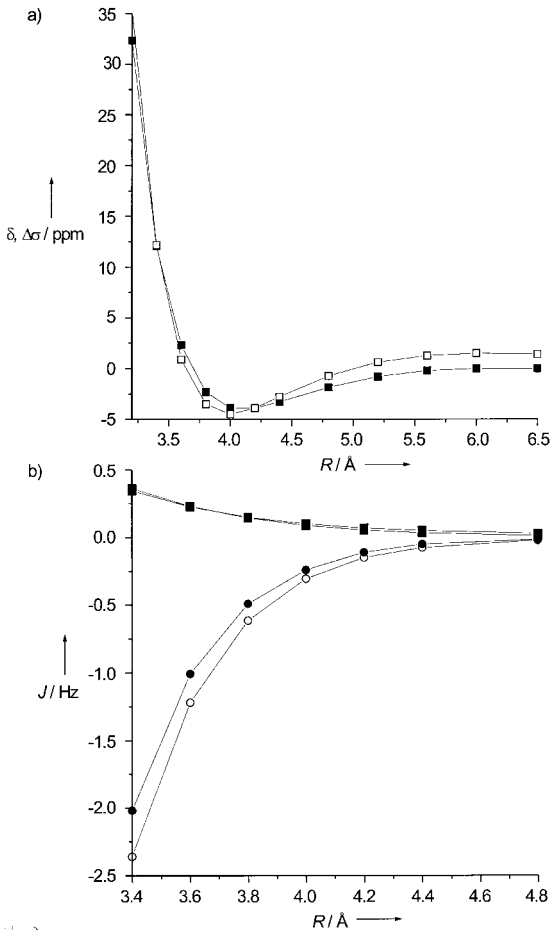

Figure 7. a) NMR shielding parameters of xenon in the Xe···benzene complex **2**. Chemical shift (■); shielding anisotropy (□). b) Coupling constants in the Xe···benzene complex. FC (○) and total coupling (●) of $J_{Xe,C}$; FC (□) and total coupling (■) of $J_{Xe,H}$.

The shielding tensor is again cylindrically symmetric; therefore $\Delta\sigma = \sigma_{\parallel} - \sigma_{\perp}$, where the parallel axis is the one connecting the xenon atom with the center of the benzene molecule. Upon approaching the benzene molecule, xenon is firstly shielded (at variance with the previous cases), until δ reaches a minimum of about -4 ppm at 4.0 Å. However, further shortening of the distance causes a deshielding, so that δ goes through zero and then becomes positive. The anisotropy has a very similar behavior and the chemical shift is largely due to a variation of $\sigma_{\perp}$, as before. We note that the sign change of the anisotropy corresponds to a change in the relative magnitude of the parallel and perpendicular component of the shielding tensor, that is, a change of the shape of the tensor from prolate (rod-like) at large separation, to oblate (disk-like) at short distances. Our results qualitatively agree with those of Bühl et al.[18] They found that xenon in the Xe···benzene complex (the Xe···benzene distance was set to the same value as in Xe@C_{60}) was deshielded by $+15$ ppm at

0947-6539/03/0907-1492 $ 20.00+.50/0 *Chem. Eur. J.* **2003**, *9*, No. 7

the MP2 level compared with the noncorrelated SCF level. The higher chemical shift at the correlated level is in qualitative agreement with the large deshielding of xenon in liquid benzene compared to the gas phase (188.14 ppm) and in fullerene (179.24 ppm).[15]

The through-space coupling constant $J_{Xe,C}$ is shown in Figure 5b. It shows a non-negligible value of a few tenths of a Hz at r_{eq}, mainly due to the FC contribution partly canceled by the PSO term. For example, at 4.0 Å the DSO, PSO, FC, SD terms are -0.02, 0.09, -0.30 and -0.01 Hz, respectively.

The Xe···(benzene)$_2$ complex (3): In this sandwich complex, for which we did not investigate the energetics due to its large size, we found again that the chemical shift and the shielding anisotropy are very close. The behavior is somewhat similar to the case of complex **2** with the only difference of a larger induced anisotropy and, in turn, a stronger chemical shift dependence on the distance (see Figure 8).

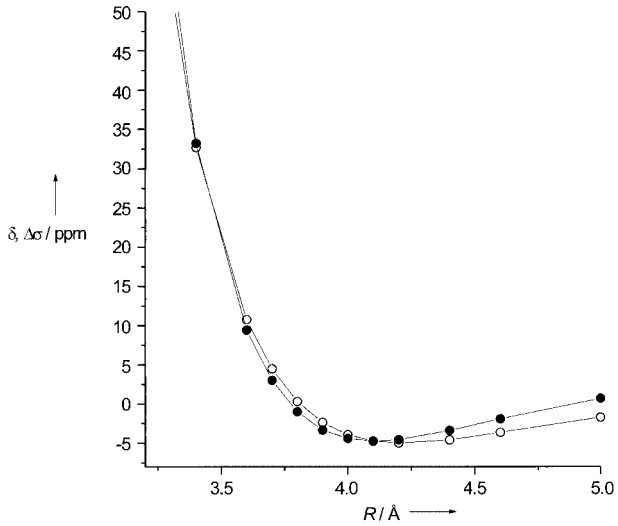

Figure 8. NMR shielding parameters in the benzene···Xe···benzene complex **3**. Chemical shift (○), shielding anisotropy (●).

Thus, for both benzene complexes **2** and **3** the anisotropy and the chemical shift exhibit a minimum. Hence, it appears that for distances longer than 4 Å the shielding effect of the benzene ring current overrides the effect of the reduced symmetry at Xe, which would result in the typical decrease in shielding.

This result is in qualitative agreement with the experimental observation of the chemical shift anisotropy of xenon in nematic liquid crystals which was found to be of the order of -10 ppm[10a] (notice the negative sign). From a more practical viewpoint, this behavior implies that, if Xe is caged within a host of this type, for certain distances there may be no appreciable xenon shift.

The Xe···O[Si(OH)$_3$]$_2$ complex (4): Finally, we have investigated the complex between xenon and a silicate residue O[Si(OH)$_3$]$_2$ **4**, as a model system for the interaction between xenon and such groups in zeolites. The silicate moiety was optimized at the B3LYP/6-31G(d) level with Gaussian 98; r_{eq} was calculated to be 3.96 Å and $\Delta E = -0.49$ kcal mol^{-1}. As found for the other complexes, the isotropic chemical shift closely matches the behavior of the chemical shift anisotropy (Figure 9), the latter being mostly determined by variation of the two perpendicular components, σ_x and σ_y. In this case the z axis is directed roughly along the O–Xe direction (due to the non-perfectly symmetrical arrangement of the OH groups, the reference system which diagonalizes the shielding tensor is not perfectly aligned with its z axis along the Xe–O direction) while the two Si atoms lie approximately in the yz plane. These results are qualitatively in agreement with experiments since xenon in zeolites is found to be deshielded, with respect to free xenon, by few tens to few hundreds of ppm, depending on several factors. However, an accurate evaluation of δ_{Xe} in zeolites must take into account the interaction of xenon with all the atoms of the cavity plus the mutual interactions among xenon atoms, which strictly depend on the loading.

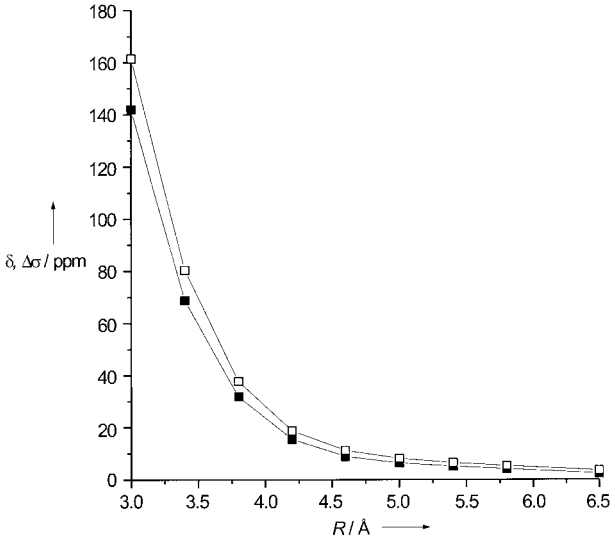

Figure 9. NMR shielding parameters of xenon in the Xe···O[Si(OH)$_3$]$_2$ complex **4**. Chemical shift (■); shielding anisotropy (□).

With regard to through-space coupling, we have calculated $J_{Xe,O}$ (with the Si-O-Si oxygen) and $J_{Xe,Si}$. Owing to the size of the complex, it was possible to run only few calculations, and the calculation of the SD term (the most time-consuming, but often the smallest term), was performed for only one distance. The results of $J_{Xe,O}$ are reported in Table 3, while we found a negligible coupling between xenon and silicon: even at a distance of 3.4 Å, $J_{Xe,Si} < 0.1$ Hz.

The main reason for this difference is the steep decrease of through-space couplings with distance; indeed, xenon is much closer to oxygen than silicon in our model system (this

Table 3. Through-space spin–spin coupling constants $J_{Xe,O}$ [Hz] at some distances for the van der Waals complex **4**.

R [Å]	DSO	PSO	FC	SD	TOT
3.4	0.05	–2.31	16.45	–	14.19
3.8	0.04	–0.96	4.63	–	3.71
4.0	0.04	–0.60	2.41	–	1.85
4.2	0.03	–0.37	1.24	0.06	0.96

  0947-6539/03/0907-1493 $ 20.00+.50/0

arrangement is somewhat forced upon, owing to the coordination mode of Si). This is confirmed by a comparison of K values, which shows that $J_{Xe,Si}$ is intrinsically very small (overriding the larger magnetogyric ratio of ^{29}Si than ^{17}O). This is unfortunate, since such small couplings would have been easier to observe between two spin-½ nuclei. Nevertheless, interestingly the $J_{Xe,O}$ through-space coupling is unusually large, of the order of few Hz in the stabilizing region, that is for distances larger than 3.48 Å, as shown in Table 3.

Conclusion

The DFT calculation of ^{129}Xe chemical shifts and spin–spin couplings in covalent compounds is feasible with good accuracy even without including relativistic effects. The use of the all-electron TZ2P basis set, at the scalar relativistic ZORA level, allows to improve the agreement with experiment; inclusion of spin–orbit coupling leads only to minor improvements, since it entails an approximately systematic correction to calculated shieldings. We have taken advantage of this capability to make predictions of the changes to be expected when Xe is located within the cavities or channels of materials commonly probed in this way. The possibility of through-space spin–spin coupling has been highlighted, and its magnitude is consistent with, or even larger than, the values computed for organic CH/π systems. Of course, many caveats apply to any such experimental verification, owing to the labile nature of these complexes. Nevertheless the detailed structural information implied by the observation of such couplings is, we believe, well worth investigating.

[1] a) C. J. Jameson in *Multinuclear NMR* (Ed.: J. Mason), Plenum Press, New York, **1987**, Chapter 18; b) M. Gerken, G. J. Schrobilgen, *Coord. Chem. Rev.* **2000**, *197*, 335.

[2] a) D. Raftery, H. Long, T. Meersman, P. J. Grandinetti, L. Reven, A. Pines, *Phys. Rev. Lett.* **1991**, *66*, 584; b) D. Raftery, L. Reven, H. Long, A. Pines, P. Tang, J. A. Reimer, *J. Phys. Chem.* **1993**, *97*, 1649; c) H. W. Long, H. C. Gaede, J. Shore, L. Reven, C. R. Bowers, J. Kritzenberger, T. Pietrass, A. Pines, P. Tang, J. A. Reimer, *J. Am. Chem. Soc.* **1993**, *115*, 8491; d) T. Room, S. Appelt, R. Seydoux, E. L. Hahn, A. Pines, *Phys. Rev. B* **1997**, *22*, 11604; e) M. Haake, A. Pines, J. A. Reimer, R. Seydoux, *J. Am. Chem. Soc.* **1997**, *119*, 11711.

[3] T. Meersmann, M. Deschamps, G. Bodenhausen, *J. Am. Chem. Soc.* **2001**, *123*, 941.

[4] a) T. Ito, J. Fraissard, *J. Chem. Phys.* **1982**, *76*, 5225; b) Q. J. Chen, J. Fraissard, *J. Phys. Chem.* **1992**, *96*, 1809.

[5] N. H. Heo, W. T. Lim, B. J. Kim, S. Y. Lee, M. C. Kim, K. Seff, *J. Phys. Chem. B* **1999**, *103*, 1881.

[6] J.-H. Yang, L. A. Clark, G. J. Ray, Y. J. Kim, H. Du, R. Q. Snurr, *J. Phys. Chem. B* **2001**, *105*, 4698.

[7] a) C. J. Jameson, *J. Chem. Phys.* **2002**, *116*, 8912; b) C. J. Jameson, H.-M. Lim, *J. Chem. Phys.* **1997**, *107*, 4373.

[8] V. Gupta, D. Kim, H. T. Davis, A. V. McCormick, *J. Phys. Chem. B* **1997**, *101*, 129.

[9] P. Sozzani, A. Comotti, R. Simonutti, T. Meersmann, J. W. Logan, A. Pines, *Angew. Chem.* **2000**, *112*, 2807; *Angew. Chem. Int. Ed.* **2000**, *39*, 2695.

[10] a) O. Muenster, J. Jokisaari, *Mol. Cryst. Liq. Cryst.* **1991**, *206*, 179; b) J. Ruohonen, J. Jokisaari, *Phys. Chem. Chem. Phys.* **2001**, *3*, 3208; c) J. Ruohonen, M. Ylihautala, J. Jokisaari, *Mol. Phys.* **2001**, *99*, 711.

[11] a) S. M. Rubin, M. M. Spence, A. Pines, D. E. Wemmer, *J. Magn. Reson.* **2001**, *152*, 79; b) S. M. Rubin, M. M. Spence, I. E. Dimitrov, E. J. Ruiz, A. Pines, D. E. Wemmer, *J. Am. Chem. Soc.* **2001**, *123*, 8616; c) E. Locci, Y. Dehouck, M. Casu, G. Saba, A. Lai, M. Luhmer, J. Reisse, K. Bartik, *J. Magn. Reson.* **2001**, *150*, 167.

[12] Y. Xu, P. Tang, *Biochim. Biophys. Acta Biomembr.* **1997**, *1323*, 154.

[13] H. E. Moller, M. S. Chawla, X. J. Chen, B. Driehuys, L. W. Hedlund, C. T. Wheeler, G. A. Johnson, *Magn. Reson. Med.* **1999**, *41*, 1058.

[14] a) T. Brotin, A. Lesage, L. Emsley, A. Collet, *J. Am. Chem. Soc.* **2000**, *122*, 1171; b) T. Brotin, T. Devic, A. Lesage, L. Emsley, A. Collet, *Chem. Eur. J.* **2001**, *7*, 1561.

[15] M. S. Syamala, R. J. Cross, M. Saunders, *J. Am. Chem. Soc.* **2002**, *124*, 6216.

[16] A. Freitag, C. v. Wüllen, V. Staemmler, *Chem. Phys.* **1995**, *192*, 267.

[17] S. Tanaka, M. Sugimoto, H. Takashima, H. Hada, H. Nakatsuji, *Bull. Chem. Soc. Jpn.* **1996**, *69*, 953.

[18] M. Bühl, S. Patchkovskii, W. Thiel, *Chem. Phys. Lett.* **1997**, *275*, 14.

[19] C. J. Jameson, A. C. de Dios, *J. Chem. Phys.* **2002**, *116*, 3805.

[20] J.-H. Kantola, J. Vaara, T. T. Rantola, J. Jokisaari, *J. Chem. Phys.* **1997**, *107*, 6470.

[21] F. R. Salsbury, R. H. Harris, *Mol. Phys.* **1998**, *94*, 307.

[22] a) A. Bagno, G. Saielli, G. Scorrano, *Angew. Chem.* **2001**, *113*, 2600; *Angew. Chem. Int. Ed.* **2001**, *40*, 2532; b) A. Bagno, G. Saielli, G. Scorrano, *Chem. Eur. J.* **2002**, *8*, 2047; c) A. Bagno, G. Saielli, G. Scorrano, *ARKIVOC* **2002**, *IV*, 38; d) A. Bagno, G. Casella, G. Saielli, G. Scorrano, *Int. J. Mol. Sci.* **2003**, in press.

[23] M. Pecul, J. Sadlej, J. Leszczynski, *J. Chem. Phys.* **2001**, *115*, 5498.

[24] I. G. Shenderovich, S. N. Smirnov, G. S. Denisov, V. A. Gindin, N. S. Golubev, A. Dunger, R. Reibke, S. Kirpekar, O. L. Malkina, H.-H. Limbach, *Ber. Bunsenges. Phys. Chem.* **1998**, *102*, 422.

[25] D. L. Bryce, R. E. Wasylishen, *Inorg. Chem.* **2002**, *41*, 3091.

[26] A. Bagno, *Chem. Eur. J.* **2000**, *6*, 2925.

[27] G. te Velde, F. M. Bickelhaupt, E. J. Baerends, C. Fonseca Guerra, S. J. A. van Gisbergen, J. G. Snijders, T. Ziegler, *J. Comput. Chem.* **2001**, *22*, 931. ADF 2002.01: http://www.scm.com

[28] a) G. Schreckenbach, T. Ziegler, *J. Phys. Chem.* **1995**, *99*, 606; b) G. Schreckenbach, T. Ziegler, *Int. J. Quantum Chem.* **1997**, *61*, 899; c) S. K. Wolff, T. Ziegler, *J. Chem. Phys.* **1998**, *109*, 895; d) S. K. Wolff, T. Ziegler, E. van Lenthe, E. J. Baerends, *J. Chem. Phys.* **1999**, *110*, 7689.

[29] a) R. M. Dickson, T. Ziegler, *J. Phys. Chem.* **1996**, *100*, 5286; b) J. Khandogin, T. Ziegler, *Spectrochim. Acta A* **1999**, *55*, 607; c) L. Autschbach, T. Ziegler, *J. Chem. Phys.* **2000**, *113*, 936; d) L. Autschbach, T. Ziegler, *J. Chem. Phys.* **2000**, *113*, 9410.

[30] N. F. Ramsey, *Phys. Rev.* **1953**, *91*, 303.

[31] a) G. Schreckenbach, T. Ziegler, *J. Phys. Chem. A* **2000**, *104*, 8244; b) L. Autschbach, T. Ziegler, *J. Am. Chem. Soc.* **2001**, *123*, 3341; c) L. Autschbach, T. Ziegler, *J. Am. Chem. Soc.* **2001**, *123*, 5320.

[32] M. Bühl, S. Gaemers, C. J. Elsevier, *Chem. Eur. J.* **2000**, *6*, 3272.

[33] a) M. Kaupp, C. Aubauer, G. Engelhardt, T. M. Klapötke, O. L. Malkina, *J. Chem. Phys.* **1999**, *110*, 3897; b) C. Aubauer, M. Kaupp, T. M. Klapötke, H. Nöth, H. Piotrowski, W. Schnick, J. Senker, M. Suter, *J. Chem. Soc. Dalton Trans.* **2001**, 1880.

[34] M. Kaupp, O. L. Malkina, V. G. Malkin, P. Pyykkö, *Chem. Eur. J.* **1998**, *4*, 118.

[35] a) N. Godbout, D. R. Salahub, J. Andzelm, E. Wimmer, *Can. J. Chem.* **1992**, *70*, 560; b) Basis sets were obtained from the extensible computational chemistry environment basis set database, Version 6/28/02, as developed and distributed by the Molecular Science Computing Facility, Environmental and Molecular Sciences Laboratory, which is part of the Pacific Northwest Laboratory, P.O. Box 999, Richland, Washington 99352 (USA), and funded by the US Department of Energy. The Pacific Northwest Laboratory is a multiprogram laboratory operated by Battelle Memorial Institute for the US Department of Energy under contract DE-AC06-76RLO 1830. Contact David Feller or Karen Schuchardt for further information.

[36] Gaussian 98 (Revision A.9), M. J. Frisch, G. W. Trucks, H. B. Schlegel, G. E. Scuseria, M. A. Robb, J. R. Cheeseman, V. G. Zakrzewski, J. A. Montgomery, Jr., R. E. Stratmann, J. C. Burant, S. Dapprich, J. M. Millam, A. D. Daniels, K. N. Kudin, M. C. Strain, O. Farkas, J. Tomasi, V. Barone, M. Cossi, R. Cammi, B. Mennucci, C. Pomelli, C. Adamo, S. Clifford, J. Ochterski, G. A. Petersson, P. Y. Ayala, Q. Cui, K.

0947-6539/03/0907-1494 $ 20.00+.50/0 *Chem. Eur. J.* **2003**, *9*, No. 7

Morokuma, D. K. Malick, A. D. Rabuck, K. Raghavachari, J. B. Foresman, J. Cioslowski, J. V. Ortiz, A. G. Baboul, B. B. Stefanov, G. Liu, A. Liashenko, P. Piskorz, I. Komaromi, R. Gomperts, R. L. Martin, D. J. Fox, T. Keith, M. A. Al-Laham, C. Y. Peng, A. Nanayakkara, M. Challacombe, P. M. W. Gill, B. Johnson, W. Chen, M. W. Wong, J. L. Andres, C. Gonzalez, M. Head-Gordon, E. S. Replogle, J. A. Pople, Gaussian, Inc., Pittsburgh PA, **1998**.
[37] S. F. Boys, F. Bernardi, *Mol. Phys.* **1970**, *19*, 553.
[38] J. M. L. Martin, A. Sundermann, *J. Chem. Phys.* **2001**, *114*, 3408.
[39] M. Kaupp, Ch. van Wüllen, R. Franke, F. Schmitz, W. Kutzelnigg, *J. Am. Chem. Soc.* **1996**, *118*, 11939.
[40] a) T. D. Crawford, K. W. Springer, H. F. Schaefer III, *J. Chem. Phys.* **1995**, *102*, 3307; b) D. Yu, Z. D. Chen, *J. Mol. Struct. (THEOCHEM)* **2001**, *540*, 29.
[41] H. Rupp, K. Seppelt, *Angew. Chem.* **1974**, *86*, 669; *Angew. Chem. Int. Ed. Engl.* **1974**, *13*, 612.
[42] R. D. Burbank, G. R. Jones, *J. Am. Chem. Soc.* **1974**, *96*, 43.
[43] S. Seidel, K. Seppelt, *Angew. Chem.* **2001**, *113*, 4318; *Angew. Chem. Int. Ed.* **2001**, *40*, 4225.
[44] P. Tsao, C. C. Cobb, H. H. Claassen, *J. Chem. Phys.* **1971**, *54*, 5247.
[45] G. J. Schrobilgen, J. H. Holloway, P. Granger, C. Brevard, *Inorg. Chem.* **1978**, *17*, 980.
[46] S. W. Peterson, R. D. Willet, J. L. Huston, *J. Chem. Phys.* **1973**, *59*, 453.
[47] N. Bartlett, M. Wechsberg, G. R. Jones, R. D. Burbank, *Inorg. Chem.* **1972**, *11*, 1124.
[48] G. A. Schumacher, G. J. Schrobilgen, *Inorg. Chem.* **1984**, *23*, 2923.
[49] 1D. H. Templeton, A. Zalkin, J. D. Forrester, S. M. Williamson, *J. Am. Chem. Soc.* **1963**, *85*, 817.
[50] J. F. Sawyer, G. J. Schrobilgen, S. J. Sutherland, *J. Chem. Soc. Chem. Commun.* **1982**, 210.
[51] F. O. Sladky, P. A. Bulliner, N. Bartlett, *J. Chem. Soc. A* **1969**, 2179.
[52] J. P. Perdew, J. A. Chevary, S. H. Vosko, K. A. Jackson, M. R. Pederson, D. J. Singh, C. Fiolhais, *Phys. Rev. B* **1992**, *46*, 6671.
[53] J. P. Perdew, K. Burke, M. Ernzerhof, *Phys. Rev. Lett.* **1996**, *77*, 3865.
[54] B. Hammer, L. B. Hansen, J. K. Norskov, *Phys. Rev. B* **1999**, *59*, 7413.
[55] Y. Zhang, W. Yang, *Phys. Rev. Lett.* **1998**, *80*, 890.
[56] A. D. Becke, *Phys. Rev. A* **1988**, *38*, 3098.
[57] C. Lee, W. Yang, R. G. Parr, *Phys. Rev. B* **1988**, *37*, 785.
[58] J. P. Perdew, *Phys. Rev. B* **1986**, *33*, 8822
[59] We note that, in any event, the observed multiplicity (broad doublet) is inconsistent with the suggested scalar coupling with ^{35,37}Cl ($I = 3/2$), since this would give rise to a 1:1:1:1 quartet. With regard to this, we would like to point out that the observed line broadening might be consistent with exchange between two unestablished species.
[60] S. A. Kafafi, *J. Phys. Chem. A* **1998**, *102*, 10404.
[61] R. A. Aziz, M. J. Slaman, *Mol. Phys.* **1986**, *57*, 825.

Received: August 30, 2002 [F4379]

  0947-6539/03/0907-1495 $ 20.00+.50/0